6ICEGE 6th International Conference on Earthquake Geotechnical Engineering
1-4 November 2015
Christchurch. New Zealand

Fabric evolution during cyclic shearing within anisotropic critical state theory for sands

A. G. Papadimitriou[1], Y. F. Dafalias[2], X. S. Li[3]

ABSTRACT

This paper studies the evolution of the fabric of sands, expressed by an appropriate deviatoric fabric tensor, during cyclic loading. The macroscopic study is performed with the aid of a simple constitutive model developed within the recently proposed anisotropic critical state theory (ACST). The model adopts the SANISAND constitutive model platform and uses a fundamental ingredient of ACST, namely the fabric anisotropy variable A that equals the first joint invariant of the evolving fabric and loading direction tensors. The study highlights the intricacies of cyclic loading and its effects on the A and the norm of the fabric tensor, as compared to the case of monotonic loading where the fabric gradually evolves towards its critical state value.

Introduction

Recent research efforts (e.g. Li and Dafalias 2012) have underlined the role of anisotropic fabric at the critical state of geomaterials. For monotonic loading, in particular, the fabric is expected to gradually evolve towards its final value (attained at critical state), but its evolution during cyclic loading is not as straightforward. Hence, this paper attempts a macroscopic study of the evolution of fabric and its importance, by employing a simple anisotropic model for sands.

The model is based on the Anisotropic Critical State Theory (ACST), which was recently proposed by Li and Dafalias (2012). This theory is combined with a model from the SANISAND constitutive model platform, an acronym term for Simple ANIsotropic SAND. The platform is based on the pioneering works of Manzari and Dafalias (1997), Dafalias and Manzari (2004) and Li and Dafalias (2000), who introduced dependence of the bounding and dilatancy model surfaces on the state parameter ψ (Been and Jefferies 1985). This innovative concept allows for the simulation of sand response irrespective of initial conditions with a single set of constants.

The paper outlines the basic concepts of ACST in section 2, and then, in section 3, it presents how this is combined with a simplified version of the (SANISAND) model of Dafalias et al. (2004). Then, section 4 presents how the model simulates undrained cyclic loading of sands. Finally, section 5 focuses on the evolution of fabric-related parameters during such loading paths and how this evolution affects the simulated response.

[1]Assist. Professor, School of Civil Engr., National Technical University of Athens, Greece, apapad@civil.ntua.gr
[2]Professor, Univ. California Davis, USA & Nation. Technical University of Athens, Greece, jfdafalias@ucdavis.edu
[3]Professor, Hong Kong University Science & Technology, Clear Water Bay, Hong Kong SAR, China, xsli@ust.hk

Anisotropic Critical State Theory

This section outlines the basic elements of the ACST of Li and Dafalias (2012). Tensors are denotes in bold, but the emphasis of the paper is set on the triaxial formulation. This is described in terms of effective stress quantities $p = (\sigma_a + 2\sigma_r)/3$, $q = (\sigma_a - \sigma_r)$ and respective strain quantities $\varepsilon_v = (\varepsilon_a + 2\varepsilon_r)$, $\varepsilon_q = 2(\varepsilon_a - \varepsilon_r)/3$, where subscripts a and r denote the axial and radial directions, while subscripts v and q denote the volumetric and deviatoric strain components. Let **F** be the (density-independent) deviatoric part of a symmetric second-order fabric tensor related to either the orientation (and shape) of the voids, or the spatial distribution of particles' contact normal directions, with proper normalization. It is given by:

$$\mathbf{F} = F\mathbf{n}_\mathbf{F} \tag{1}$$

where F is the norm of the tensor and $\mathbf{n}_\mathbf{F}$ the unit-norm deviatoric tensor denoting its direction. For axisymmetric sand fabric (usual for deposition under gravity), the principal values of **F** are only two, F_1 and F_2=F_3, and the norm F is equal to:

$$F = (2/3)^{0.5}\left|F_1 - F_2\right| \tag{2}$$

With **n** being the unit-norm deviatoric tensor denoting the loading direction, usually defined along the deviatoric plastic strain rate, the scalar Fabric Anisotropy Variable (FAV) A is:

$$A = \mathbf{F} : \mathbf{n} = FN \tag{3}$$

where **:** denotes the trace of the product of adjacent tensor and $N = \mathbf{n}_\mathbf{F} : \mathbf{n}$ is the measure of the relative orientation of **F** versus **n**. In the triaxial stress space, the **n** may be defined as a scalar s that takes values +1 and –1 for loading towards triaxial compression (TC) and triaxial extension (TE), respectively. Similarly, the fabric direction in triaxial space may be defined in terms of a scalar s_F corresponding to the sign of $\mathbf{n}_\mathbf{F}$, thus, taking values +1 when $F_1 > F_2$ for triaxial compression like (tcl) fabric structures, and –1 when $F_1 < F_2$ for triaxial extension like (tel) structures. Hence, in the triaxial stress space it follows that $N = s\ s_F$, while one may define a directional (triaxial) norm $F' = F\ s_F$ (where $F'=F > 0$ in tcl fabric and $F' = -F < 0$ in tel fabric).

According to ACST, the **F** is expected to evolve during (plastic only) loading towards **n** at critical state. Thus, the normalized value of F evolves towards 1.0, while the $\mathbf{n}_\mathbf{F}$ towards **n**. Assuming that the maximum value of F is 1.0 and attained only at critical state, its evolution rate equation from its initial value F_{in} (a model constant) to 1.0, reads

$$\dot{F} = \langle L \rangle c(N - F) \tag{4}$$

with c depicting the rate of fabric evolution during loading. Due to gravitational deposition, usually $0 < F_{in}' = F_{in} < 1$ (tcl fabric), and hence loading towards TC would lead to an increase of F (since $N = 1$, rendering $\dot{F} > 0$) and consequently to an increase of A (as well as F and F') from its initial positive value $A = F_{in}$ towards its peak value $A = 1.0$ at critical state (where also $F = F' = 1.0$). On the other hand, loading of a tcl fabric structure towards TE would lead initially to a decrease of F (since $N = -1$, rendering $\dot{F} < 0$) and consequently to an algebraic increase of A (due to $N = -1$) from its initially negative value $A = -F_{in}$ up to zero and finally to $A = 1.0$, again.

In other words, continuation of the loading towards TE without change of direction, eventually aligns the $\mathbf{n_F}$ with $\mathbf{n}$ along TE, thus, making $N = 1$ and leading F towards 1.0. Then $\dot{F} = 0$ (due to $N = F$ in Eq. 4) while $A = 1.0$ and critical state is reached, but with $F' = -1.0$ this time.

It should be underlined here that the foregoing condition expressed by $A = 1.0$ is considered in Li and Dafalias (2012) to be a third condition when attaining the critical state, concurrent to the other two conditions of the isotropic critical state theory on critical stress and void ratios. Furthermore, the A is used to define a Dilatancy State Line (DSL) in the *e-p-A* space, which delineates the dilative or contractive state of the soil, as does the Critical State Line (CSL) in isotropic critical state theory. The distance of the current void ratio e from the one on the DSL at the same p is named the Dilatancy State Parameter (DSP) ζ and is defined by:

$$\zeta = (e - e_c) - e_A(A-1) = \psi - e_A(A-1) \tag{5}$$

where e_c is the critical void ratio on the CSL at current p, $\psi = (e - e_c)$ is the state parameter of Been and Jefferies (1985), the A is as defined in Eq. (3), and the quantity $-e_A(A-1)$ depicts the ever-current downward parallel translation of the DSL in comparison to the constant CSL (see Fig. 1). The e_A (a positive model constant, for simplicity) quantifies this translation. Note that states with $\zeta > 0$ and $\zeta < 0$ correspond to contractive and dilative soil response, respectively, i.e. playing the role of ψ in isotropic critical state theory. Observe, that the DSL becomes identical to the CSL only when $A = 1.0$, i.e. at critical state, and consequently the DSP $\zeta = \psi$. In this respect, the DSP ζ may be considered an anisotropic state parameter, with ψ its isotropic counterpart.

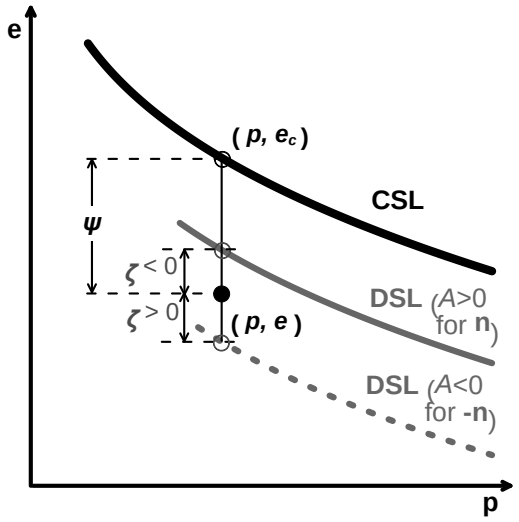

Figure 1. Effect of load reversal on the location of the DSL (and the value of ζ) in the *e-p* space (based on Li & Dafalias 2012)

Given Eqs (3) and (4), the A values in TE are generally expected to be algebraically smaller than in TC for the usual gravitational (tcl) fabrics. Based on Eq. (5), and given that $e_A > 0$, this translates to algebraically larger ζ values in TE than in TC. In other words, according to the ACST of Li and Dafalias (2012), loading in TE is expected to be more contractive than in TC, an event that is repeatedly confirmed by experiments (e.g. Yoshimine et al. 1998). Finally, based on Fig. 1, consider a case where the current values of $\mathbf{F}$ and $\mathbf{n}$ specify $A > 0$, according to Eq. (3), corresponding to $\zeta < 0$ on the basis of Eq. (5). Then, if the loading is reversed, the $\mathbf{n}$ becomes $\mathbf{-n}$,

and hence the A becomes $-A$ on the basis of Eq. (3). This leads to a relocation of the DSL lower in the e-p space, thus algebraically increasing the value of ζ, and possibly even to values of $\zeta > 0$ on the basis of Eq. (5), as shown in Fig. 1. Hence, even if the mean stress p, the void ratio e and the state parameter ψ remain constant, the response may switch from dilative ($\zeta < 0$) to contractive ($\zeta > 0$), merely due a reversal of loading, a very important aspect of the response for cyclic loading paths.

SANISAND with Evolving Fabric Anisotropy

It should be underlined that the ACST can be combined with any constitutive model platform constructed within classical isotropic critical state theory (CST). Here, this is done by adopting the SANISAND model framework, and specifically its version presented by Dafalias et al. (2004) after stripping its constitutive equations from their dependence on inherent fabric anisotropy. For brevity, Table 1 presents only the equations related to the incorporation of the ACST in the SANISAND framework. Further details can be found in the 2004 paper.

Table 1. SANISAND constitutive model equations affected by evolving fabric anisotropy

Parameter	SANISAND CST framework	SANISAND ACST framework
Bounding stress ratio	$M^b = M \exp(-n^b \psi)$	$M^b = M \exp(-n^b \zeta)$
Dilatancy stress ratio	$M^d = M \exp(n^d \psi)$	$M^d = M \exp(n^d \zeta)$

Observe in Table 1 the simplest possible incorporation of ACST in a SANISAND framework, i.e. the mere replacement of the (isotropic) state parameter ψ (set to affect the bounding and dilatancy stress ratios M^b and M^d) by its anisotropic counterpart ζ (defined in Eq. 5). This replacement is consistent with the basic assumption of the classical isotropic CST framework, that when the critical state is reached $\psi = 0$, leading to $M^b = M^d = M$. This because, when critical state is reached within the anisotropic framework, the FAV $A = 1$, and hence $\zeta = \psi = 0$ (from Eq. 5) which again leads to $M^b = M^d = M$.

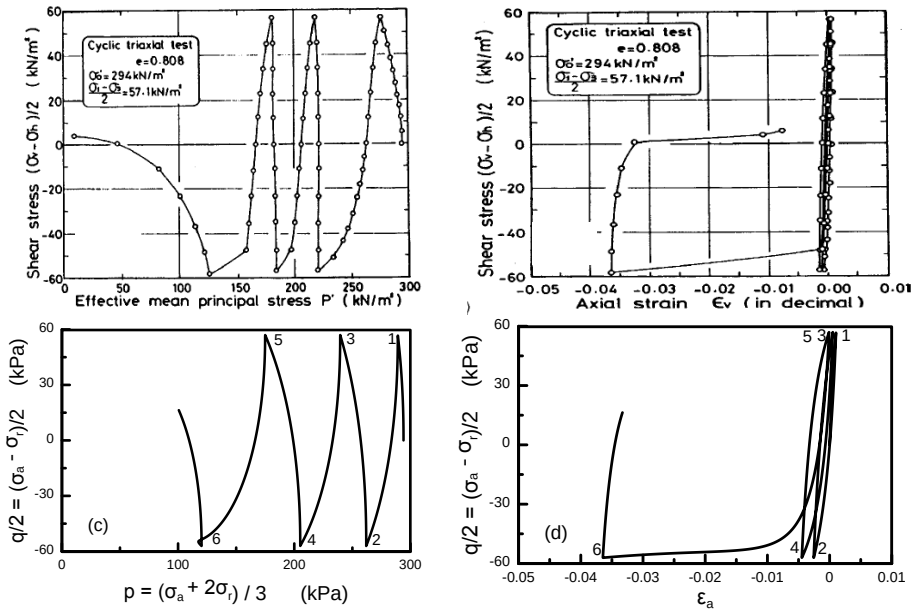

Figure 2. Effective stress path and stress-strain response of Toyoura sand in an exemplary undrained cyclic triaxial test: (a, b) data from Ishihara et al. (1975), (c, d) model simulations

Figure 2 presents an exemplary comparison of the simulation with this simple anisotropic model with data on Toyoura sand (Ishihara et al. 1975) from an undrained cyclic triaxial test with few cycles to liquefaction. The simulation was performed by setting $c = 13$, $e_A = 0.0818$ and $F_{in} = 0.5$ (initially anisotropic fabric), and its comparison to the data shows close agreement.

Cyclic model simulations of similar quality may be achieved for different initial and loading conditions (e.g. simple shear) of the same sand with the same set of constants. This is due to the fact that the hereby presented fabric evolution scheme is mounted on the SANISAND model platform, and therefore it inherits its pertinent merits. However, such simulations are not presented here due to page limitations, and mainly because the emphasis of this paper is to study the evolution of fabric during such loading paths, as discussed in the next section.

Evolution of Fabric during Cyclic Loading

Of interest here, is to study the evolution of the FAV A (of Eq. 3) and of the directional (triaxial) norm $F' = F\, s_F$ during this cyclic path. This is performed in Fig. 3, where the enumerations 1 through 6 correspond to the load reversal points indicated in Fig. 2 and aid in interpreting the complex mechanisms of fabric evolution. The following observations may be done:

a) At each load reversal, the A changes sign (from 1 to 1′, from 2 to 2′, etc.), but the directional norm F' (as well as its absolute value F) do not. The change of sign of A is related to the change of s_F from +1 to –1 and the opposite, and does not affect the value of F (see Eq. 3).
b) During the semi-cycles towards TC (consolidation to 1, 2 to 3, 4 to 5) the directional norm F' (as well as the F itself) increases in value, and so does the A. The increase of F is related to the positive sign of the $(N – F) = (1 – F)$ term in Eq. 4, which is reflected to an increase of A (since $N = s_F\, s = (+1)(+1) = 1$ during these paths).
c) On the contrary, during the semi-cycles towards TE (1 to 2, 3 to 4, 5 to 6) the directional norm F' decreases in value. This is due to a decrease of F, arising from the negative sign of the $(N – F) = (–1 – F)$ term in Eq. 4 (since $N = s_F\, s = (+1)(–1) = –1$). However, this decrease may bring the F' to zero (see path 5 to 6) and continued evolution to algebraically lower values, arising from an increase of F (since $(N – F) = (1 – F) > 0$, due to $N = (–1)(–1) = 1$).
d) Accordingly, during these semi-cycles towards TE, the FAV A algebraically increases in value, and this is due to a combination of s= –1 with the decreasing positive F' (described above). This algebraic increase continues even when the F' becomes negative (as during path 5 to 6), since it leads to a positive A value even during loading towards extension.
e) Given the successive increases (in semi-cycles in TC) and decreases (in semi-cycles in TE) of the directional norm F', the result within each cycle is a net decrease of its value. This is due to the fact that the $(N – F)$ term in Eq. (4) is larger, in absolute terms, in the TE semi-cycles than in their TC counterparts. For example, when the F' (and F) is approximately 0.4 (e.g. at point 4), then $|N – F| = |1 – F| = 0.6$ in TC, while $|N – F| = |– 1 – F| = 1.4$ in TE.
f) Among the successive semi-cycles of loading, the largest change in F' is observed in the TE semi-cycle from 5 to 6. This large change of F' occurs concurrently with a large accumulation of axial strain ε_a towards extension (of almost 3.6%). The former change is due to the latter, since the term $\langle L \rangle$ in the rate of norm F (Eq. 4) is equal, in this formulation, to the absolute value of the plastic deviatoric strain increment, which becomes highest during this TE semi-cycle.

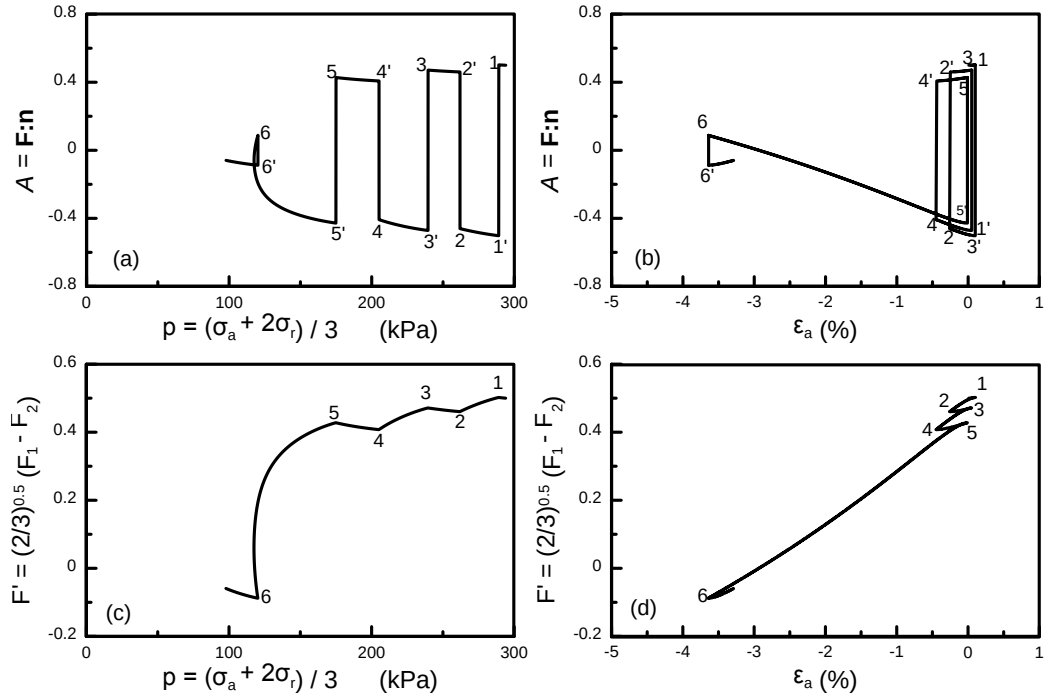

Figure 3. Illustration of fabric evolution for the model simulation of Fig.2: (a, b) evolution of FAV A as a function of p and ε_a, (c, d) evolution of F' as a function of p and ε_a

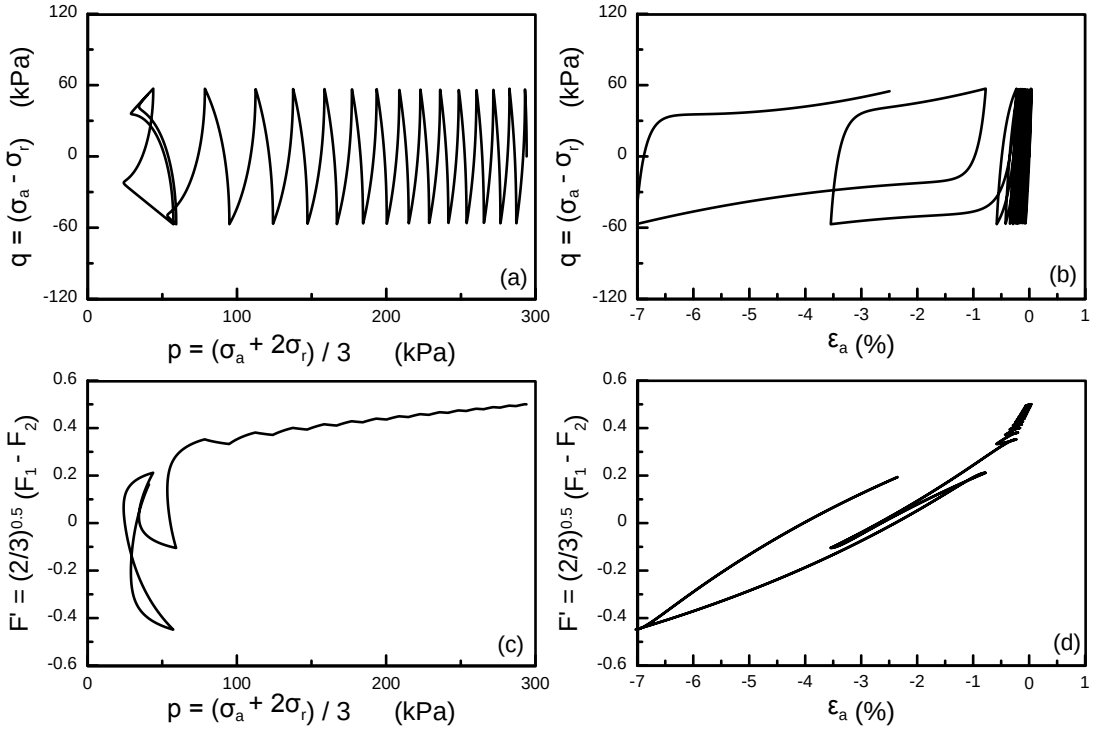

Figure 4: Response and fabric evolution during an undrained cyclic test with numerous cycles to liquefaction: (a, b) effective stress path and stress-strain response, (c, d) evolution of F' as a function of p and ε_a

These indicative results were obtained for a cyclic undrained triaxial test with a high cyclic stress ratio CSR = 57.1/294 = 0.19 leading to liquefaction in few cycles (namely 3). It would be interesting to see whether these results also hold for cyclic loading with a reduced (by 50%) CSR value and this is studied in Fig. 4. This figure shows the simulated response, but emphasizes on the F' evolution (and not of A, which is additionally affected by the load reversals making its interpretation less straightforward). Based on Fig. 4, the following conclusions may be drawn:

a) Fabric evolution during numerous cycles retains the basic characteristics outlined above, namely the gradual decrease of F' with cycles and the intense decrease of F' to values less than zero for the first time during a semi-cycle towards TE related to a large accumulated axial deformation ε_a.
b) On top of the above, at cyclic mobility (where the effective stress path essentially stabilizes in the very low stress regime) the directional norm F' also evolves significantly within each cycle due to the very large deviatoric strains produced.
c) For the example at hand, the range of F' variation within each cycle at cyclic mobility is from 0.2 (at the highest q = 57.1kPa) to –0.45 (at the lowest q = –57.1kPa), i.e. it passes through zero twice and exhibits a remarkable variation denoting intense fabric changes.

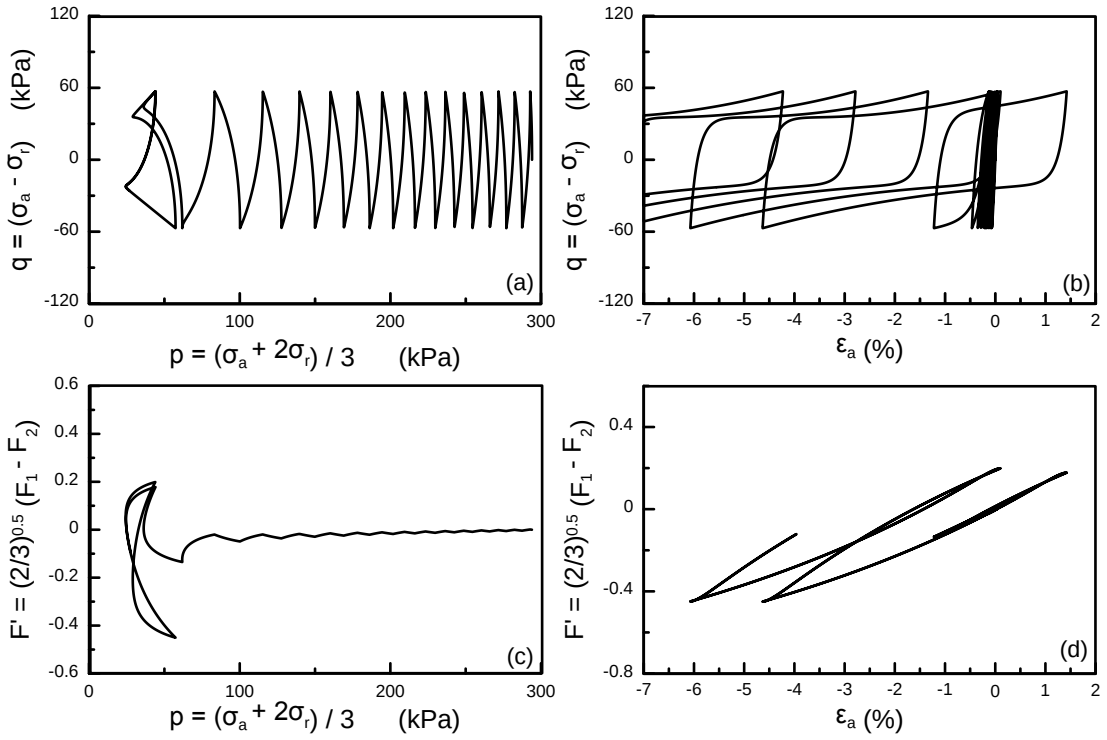

Figure 5: Effect of initial fabric isotropy (F_{in} = 0) on the response and fabric evolution during an undrained cyclic test with numerous cycles to liquefaction: (a, b) effective stress path and stress-strain response, (c, d) evolution of F' as a function of p and ε_a

Finally, in order to study potential changes in the simulated response and the fabric evolution process in the case of an initially isotropic fabric, the same loading is simulated with this model by retaining all constants the same, but setting F_{in} = 0 (instead of 0.5). These results are presented in Fig. 5, in the format of Fig. 4, and the following observations were made:

a) The effective stress path is not much affected by the initial fabric anisotropy (e.g. liquefaction occurs in 14 cycles in both cases). However, the stress-strain response is more affected and the accumulation of strains towards the extension side is less intense (since the initial fabric is no longer aligned horizontally).
b) The F' retains the tendency to gradually reduce with cycles, but at a less intense rate. At cyclic mobility, the directional norm F' evolves again significantly within each cycle due to the very large deviatoric strains produced.
c) Interestingly, the range of F' variation within each cycle at cyclic mobility is again from 0.2 (at q = 57.1kPa) to –0.45 (at q = –57.1kPa), i.e. exactly as for F_{in} = 0.5. In other words, the intense fabric changes at very low stresses seem essentially independent of the initial fabric anisotropy. However, the amount of F' variation in this regime is not sand-specific, but is expected to be a function of other state (e.g. density) and loading (e.g. CSR) parameters.

Conclusions

This paper studies the evolution of the (deviatoric) fabric of sands during cyclic loading, with the aid of a simple model developed within the recently proposed anisotropic critical state theory (ACST: Li and Dafalias 2012). The model adopts the SANISAND constitutive model platform and uses a fundamental ingredient of ACST, namely the fabric anisotropy variable A that equals the first joint invariant of the evolving fabric **F** and loading direction **n** tensors. It is shown capable of modeling the cyclic undrained triaxial response of Toyoura sand, and it is used for studying the evolution of A and of the directional (triaxial) norm F' of the fabric tensor.

Most important conclusions include that cyclic loading of gravitational triaxial compression like fabrics leads to a gradual decrease of F', i.e. a gradual loss of the initial anisotropy. The rate of F' decrease is governed by the amplitude of the plastic deviatoric strain rate (by definition), and becomes more intense in semi-cycles towards extension rather than compression. This cycle-by-cycle decrease may eventually lead to negative values of F', i.e. a realignment of the fabric in the vertical direction (triaxial extension like fabric). During cyclic mobility, the directional norm F' evolves significantly due to the very large deviatoric strains produced, usually passing twice through zero within each cycle. The actual range of F' variation during cyclic mobility is not affected by the initial fabric anisotropy.

Acknowledgment

The research leading to these results has received funding from the European Research Council under the European Union's Seventh Framework Program FP7-ERC-IDEAS Advanced Grant Agreement n° 290963 (SOMEF) and partial support by NSF project CMMI-1162096.

References

Been, K. & Jefferies, M.G. 1985. A state parameter for sands. *Geotechnique* **35**(2): 99–112

Dafalias, Y.F. & Manzari, M.T. 2004. Simple plasticity sand model accounting for fabric change effects. *Journal of Engineering Mechanics, ASCE* **130**(6): 622–634

Dafalias, Y.F., Papadimitriou, A.G., & Li, X.S. 2004. Sand plasticity model accounting for inherent fabric anisotropy. *Journal of Engineering Mechanics, ASCE* **130**(11): 1319–1333

Ishihara, K., Tatsuoka F. & Yasuda S. 1975. Undrained deformation and liquefaction of sand under cyclic stresses.

Soils and Foundations **15**(1): 29-44

Li, X.S. & Dafalias, Y.F. 2000. Dilatancy for cohesionless soils. *Geotechnique* **50**(4): 449–460

Li, X.S. & Dafalias, Y.F. 2012. Anisotropic critical state theory: Role of fabric. *Journal of Engineering Mechanics, ASCE* **138**(3): 263–275

Manzari, M.T. & Dafalias, Y.F. 1997. A critical state two-surface plasticity model for sands. *Géotechnique* **47**(2): 255–272

Yoshimine, M., Ishihara, K. & Vargas, W. 1998. Effects of principal stress direction and intermediate principal stress on undrained shear behavior of sand. *Soils and Foundations* **38**(3): 177–186.